

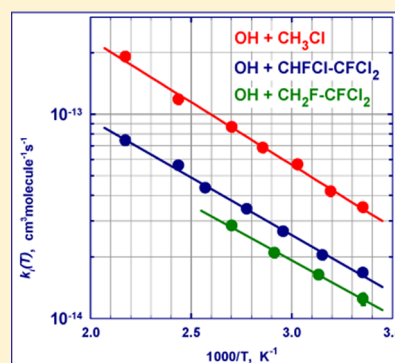
# Photochemical Properties of Some Cl-Containing Halogenated Alkanes

V. L. Orkin,<sup>\*,†,‡</sup> V. G. Khamaganov,<sup>†,‡,§</sup> E. E. Kasimovskaya,<sup>†,&</sup> and A. G. Guschin<sup>†,||</sup>

<sup>†</sup>Institute of Energy Problems of Chemical Physics, Russian Academy of Sciences, Moscow 117829, Russia

<sup>‡</sup>National Institute of Standards and Technology, Gaithersburg, Maryland 20899, United States

**ABSTRACT:** Rate constants for the gas-phase reactions of OH radicals with three partially halogenated alkanes, CH<sub>3</sub>Cl ( $k_{MC}$ ), CHFClCFCl<sub>2</sub> ( $k_{122a}$ ), and CH<sub>2</sub>FCFCl<sub>2</sub> ( $k_{132c}$ ), were measured using a discharge flow–electron paramagnetic resonance technique over the temperature range from 298 to 460 K. The temperature dependences of the rate constants can be represented by the expressions  $k_{MC}(298–460\text{ K}) = (3.09 \pm 0.94) \times 10^{-12} \exp[-(1411 \pm 85)/T] \text{ cm}^3 \text{ molecule}^{-1} \text{ s}^{-1}$ ,  $k_{122a}(298–460\text{ K}) = (1.26 \pm 0.24) \times 10^{-12} \exp[-(1298 \pm 66)/T] \text{ cm}^3 \text{ molecule}^{-1} \text{ s}^{-1}$ , and  $k_{132c}(298–370\text{ K}) = (8.1 \pm 2.2) \times 10^{-13} \exp[-(1247 \pm 89)/T] \text{ cm}^3 \text{ molecule}^{-1} \text{ s}^{-1}$ . The atmospheric lifetimes of CH<sub>3</sub>Cl, CHFClCFCl<sub>2</sub>, and CH<sub>2</sub>FCFCl<sub>2</sub> due to their reaction with OH were estimated to be 1.6, 3.5, and 4.5 years, respectively. The UV absorption cross sections of halogenated ethanes, CHFClCFCl<sub>2</sub>, and CH<sub>2</sub>FCFCl<sub>2</sub>, were measured at  $T = 295\text{ K}$  between 190 and 240 nm, as were those for CHCl<sub>2</sub>CF<sub>2</sub>Cl (HCFC-122), CHCl<sub>2</sub>CF<sub>3</sub> (HCFC-123), CHFClCF<sub>2</sub>Cl (HCFC-123a), and CH<sub>3</sub>CFCl<sub>2</sub> (HCFC-141b). The atmospheric lifetimes due to stratospheric photolysis were also estimated.



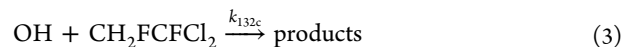
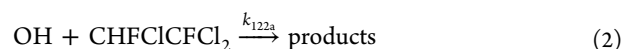
## 1. INTRODUCTION

Chlorinated alkanes are the primary sources of chlorine in the stratosphere. The potential impact of a compound on the stratospheric ozone layer is dictated by the competition between its removal in the troposphere and its destruction in the stratosphere to release Cl atoms. The major removal process for such compounds in the troposphere is reaction with OH radicals, which dictates their atmospheric lifetimes, although wet deposition and dissolution in the ocean can contribute as well. UV photolysis in the stratosphere has only a minor effect on the total atmospheric lifetime of partially halogenated alkanes. However, it contributes to their decomposition in the stratosphere to release Cl atoms, which initiate the catalytic process of ozone destruction. Thus, OH reaction rate constants and UV absorption spectra of such compounds are needed to estimate their potential environmental impact.

Methyl chloride (CH<sub>3</sub>Cl) is the most abundant chlorine-containing organic compound in the atmosphere. Methyl chloride is of natural origin, with a measured atmospheric concentration (mixing ratio) of 0.55 ppbV and an estimated emission rate exceeding 4 MT/year.<sup>1</sup> With a relatively long total residence time in the atmosphere, methyl chloride appears to be the main natural source of chlorine in the stratosphere, thereby dictating the natural level of chlorine in this region of the atmosphere. Accurate photochemical parameters of methyl chloride allow estimation of its ground emission rate based on field observations of its concentration in the atmosphere. Various other chlorine-containing halogenated compounds can appear in chemical manufacturing as intermediate or target products. Some of these were considered as potential

chlorofluorocarbon (CFC) substitutes and are controlled under the Montreal Protocol and its amendments.

In this article, we present the results of rate constant measurements for reactions of OH with methyl chloride, 1,1,2-trichloro-1,2-difluoroethane (HCFC-122a), and 1,1-dichloro-1,2-difluoroethane (HCFC-132c)



Reaction 1 has been the subject of numerous studies since 1976, whereas only one study of reaction 2 has been published and no data on reaction 3 are available.<sup>2</sup> We also present UV absorption spectra of several Cl-containing halogenated ethanes, namely, CHFClCFCl<sub>2</sub> (HCFC-122a), CH<sub>2</sub>FCFCl<sub>2</sub> (HCFC-132c), CHCl<sub>2</sub>CF<sub>2</sub>Cl (HCFC-122), CHFClCF<sub>2</sub>Cl (HCFC-123a), CHCl<sub>2</sub>CF<sub>3</sub> (HCFC-123), and CH<sub>3</sub>CFCl<sub>2</sub> (HCFC-141b), measured between 190 and 240 nm at  $T = 295\text{ K}$ . No UV absorption data are available in the literature for the first four compounds.<sup>2</sup>

## 2. EXPERIMENTAL SECTION<sup>3</sup>

### 2.1. OH Reaction Rate Constant Measurements.

Detailed descriptions of the apparatus and the experimental

Received: January 13, 2013

Revised: May 29, 2013

Published: May 31, 2013

methods employed in the present work are given elsewhere.<sup>4</sup> Thus, only a brief overview is provided here. The principal component of the discharge flow–electron paramagnetic resonance (DF/EPR) apparatus is a quartz tubular reactor of 2.0 cm i.d. coated internally with in-situ polymerized perfluorinated fluorocarbon varnish (F-46) to reduce wall loss of OH and to prevent heterogeneous reactions. The temperature of the reactor was controlled ( $\pm 0.3$  K) with water (298–370 K) or mineral oil (410 and 460 K) circulated through its outer jacket. Hydrogen atoms were generated by microwave discharge (2.45 GHz, 10–20 W) in a H<sub>2</sub>/He mixture flowing through the movable quartz injector. OH radicals were produced in the flow reactor near the end of this injector through the fast reaction between H atoms and NO<sub>2</sub>. Both NO<sub>2</sub> and the reactant (halogenated alkane under study) were injected into the flow reactor upstream of the injector tip. They were always in large excess over the hydroxyl radicals in the reactor. The OH concentration was monitored using EPR spectroscopy at the end of the flow reactor. The initial OH concentration in this study ranged from  $2 \times 10^{11}$  to  $2 \times 10^{12}$  molecules/cm<sup>3</sup>. The average linear gas flow velocity ( $v$ ) in the reactor was 6–15 m/s, at a total gas pressure of 0.4 kPa (3.0 Torr). The total pressure was measured at both ends of the reactor. Flow rates of all gases were determined by direct measurements of the rate of the pressure change in calibrated volumes. The overall instrumental uncertainty of the measurements was estimated to be less than 7%. The decay rate of OH was measured by varying the distance,  $z$  (4–30 cm), between the movable injector and the cavity of the EPR spectrometer. The OH loss rate coefficients ( $k'$ ) at any fixed reactant concentration,  $[RH]$ , were obtained from the equation

$$k' = v \frac{d}{dz} \ln \frac{[OH]_0}{[OH](z)} \quad (4)$$

where  $[OH](z)$  and  $[OH]_0$  are hydroxyl concentrations (EPR signals) at  $z$  and  $z = 0$ , respectively. The thus-obtained  $k'$  value was slightly corrected for the axial diffusion to obtain the pseudo-first-order rate coefficients,  $k$ , using the expression

$$k = k' \left( 1 + k' \frac{D}{v^2} \right) \quad (5)$$

where  $D$  is the OH diffusion coefficient. Finally, the bimolecular rate constant,  $k_b$ , at a particular temperature was derived from the slope of a plot of  $k$  versus the halogenated alkane concentration,  $[RH_i]$ , using the expression

$$k = k_w + k_i[RH_i] \quad (6)$$

where  $k_w$  is the first-order OH decay rate due to its heterogeneous removal in the absence of the reactant and  $k_i$  is the bimolecular rate constant for the reaction under study. The technique was described in detail in ref 4 and the references therein.

**2.2. UV Absorption Cross Section Measurements.** The UV absorption cross sections over the wavelength range of 190–240 nm were measured using two double-beam diffraction spectrophotometers: a Shimadzu UV-3100 spectrophotometer and a spectrometric system based on the hardware of a Specord M-40 spectrophotometer.<sup>5</sup> Each spectrum was recorded with an increment of 0.05–0.5 nm and a spectral slit width ranging from 0.1 to 1.0 nm. The pressure inside the absorption cell was measured with a bellows manometer with an accuracy of ca.  $\pm 1.3$  Pa (0.01 Torr). The results presented here were obtained

by using a  $14.0 \pm 0.05$  cm quartz cell thermostatted at 295 K. The test experiments were performed with 4.7- and 9.4-cm-long absorption cells to check the potential effect of compound adsorption at the optical windows. Comparison between the spectrum of the evacuated cell and the spectrum of the cell filled with 101 kPa (760 Torr) of xenon showed no effect of molecular refraction on the results, especially at lower absorption. Absorption spectra of the evacuated cell and of the cell filled with a Cl-containing compound were alternately recorded several times, and the absorption cross sections were calculated from their difference. There were no deviations from the Beer–Lambert law when the absorbance was less than ca. 1.0. Cross sections over each spectral interval of measurements were determined from the slopes of plots of the measured absorbance versus compound concentration. The overall instrumental error resulting from uncertainties in the path length, pressure, temperature, and measured absorbance was estimated to be less than 2% over most of wavelength range. It increases at the longest wavelengths when a very low absorption is measured at the largest concentrations of a compound with no test experiments at various pressures.

**2.3. Materials.** The samples of halogenated alkanes used in this study were provided by the Institute of Chemical Technology, Moscow, Russia: methyl chloride, CH<sub>3</sub>Cl (stated purity of >99.9% with traces of water and no detected organic impurities); CHFCl–CFCl<sub>2</sub>, HCFC-122a (>99.74%; the isomer CHCl<sub>2</sub>–CF<sub>2</sub>Cl was the main impurity, 0.23%); CH<sub>2</sub>F–CFCl<sub>2</sub>, HCFC-132c (>99.9%, no detected impurities). Another sample of CHFCl–CFCl<sub>2</sub> (>98.3%; the isomer CHCl<sub>2</sub>–CF<sub>2</sub>Cl was the main impurity) was provided by the State Institute of Applied Chemistry, St. Petersburg, Russia. All samples were carefully degassed through multiple freeze–pump–thaw–boil cycles. The carrier flow gas, He, was 99.999% pure, and H<sub>2</sub> was 99.98% pure.

The samples of CHCl<sub>2</sub>CF<sub>2</sub>Cl, HCFC-122 (>99.6%); CHCl<sub>2</sub>–CF<sub>3</sub>, HCFC-123 (>99.7%); CHFClCF<sub>2</sub>Cl, HCFC-123a (>99.9%); and CH<sub>3</sub>CFCl<sub>2</sub>, HCFC-141b (>99.9%) for UV absorption cross section measurements were provided by the State Institute of Applied Chemistry.

### 3. RESULTS AND DISCUSSION

**3.1. OH Reaction Rate Constants.** The rate constants determined for the title reactions are presented in Table 1 and Figures 1 and 2. The Arrhenius parameters derived from the fit to the experimental data are presented in Table 2 for comparison with the available results.

**3.1.1. CH<sub>3</sub>Cl (Methyl Chloride).** Figure 1 shows all of the available data for this reaction below 500 K. The data obtained in this work are shown as solid circles and an Arrhenius fit to our data yields following expression:

$$k_{MC}(298\text{--}460\text{ K}) = (3.90 \pm 0.94) \times 10^{-12} \exp[-(1411 \pm 85)/T] \text{ cm}^3 \text{ molecule}^{-1} \text{ s}^{-1} \quad (7)$$

This expression is shown in Figure 1 with the solid line extended well beyond the temperature range of measurements. The 95% confidence intervals of this dependence are shown with dashed lines. The room-temperature rate constant derived from the fit to the entire data set is

$$k_{MC}(298\text{ K}) = (3.43 \pm 0.18) \times 10^{-14} \text{ cm}^3 \text{ molecule}^{-1} \text{ s}^{-1} \quad (8)$$

**Table 1.** Rate Constants Measured for Reactions of OH with  $\text{CH}_3\text{Cl}$ ,  $\text{CHClCFCl}_2$  (HCFC-122a), and  $\text{CH}_2\text{FCFCl}_2$  (HCFC-132c)<sup>a</sup>

<i>T</i> (K)	<i>k</i> <sub>MC</sub> ( <i>T</i> ) (×10 <sup>14</sup> cm <sup>3</sup> molecule <sup>−1</sup> s <sup>−1</sup> )	<i>k</i> <sub>122a</sub> ( <i>T</i> ) (×10 <sup>14</sup> cm <sup>3</sup> molecule <sup>−1</sup> s <sup>−1</sup> )	<i>k</i> <sub>132c</sub> ( <i>T</i> ) (×10 <sup>14</sup> cm <sup>3</sup> molecule <sup>−1</sup> s <sup>−1</sup> )
298	3.36 ± 0.17 (56)	1.67 ± 0.05 (33)	1.24 ± 0.08 (9)
313	4.02 ± 0.20 (9)		
317		2.04 ± 0.09 (24)	
319			1.63 ± 0.02 (4)
330	5.44 ± 0.27 (8)		
338		2.66 ± 0.10 (10)	
343			2.09 ± 0.09 (7)
350	6.57 ± 0.33 (9)		
360		3.42 ± 0.12 (55)	
370	8.31 ± 0.42 (98)		2.83 ± 0.08 (20)
389		4.35 ± 0.13 (31)	
410	11.3 ± 0.6 (12)	5.59 ± 0.21 (18)	
421			
460	18.4 ± 0.9 (13)	7.41 ± 0.26 (31)	

<sup>a</sup>Uncertainties are two standard errors from the least-squares fit of a straight line to the measured OH decay rates versus the reactant concentrations and do not include the estimated instrumental uncertainty of 7%. The number of experiments for each temperature is shown in parentheses.

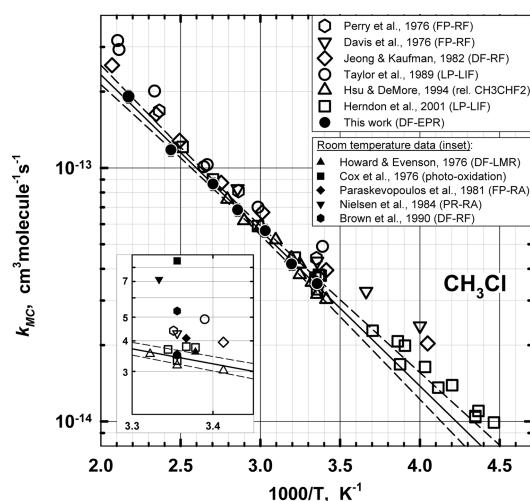


**Figure 1.** Results of rate constant measurements for the reaction between OH and  $\text{CH}_3\text{Cl}$ : (▲) Howard and Evenson,<sup>12</sup> (■) Cox et al.,<sup>13</sup> (○) Perry et al.,<sup>6</sup> (▽) Davis et al.,<sup>7</sup> (◆) Paraskevopoulos et al.,<sup>14</sup> (◇) Jeong and Kaufman,<sup>8</sup> (▼) Nielsen et al.,<sup>15</sup> (○) Taylor et al.,<sup>9</sup> (●) Brown et al.,<sup>16</sup> (△) Hsu and DeMore,<sup>10</sup> (□) Herndon et al.,<sup>11</sup> (●) this study. Lines show the results of the least-squares fit to our data (solid) and its 95% confidence intervals (dashed).

The uncertainties in both expressions 7 and 8 are two standard errors from the least-squares fit to the data and do not include the estimated instrumental uncertainty of less than 7%.

Six studies of the temperature dependence of this reaction have been published.<sup>6–11</sup> The results of these studies are shown in Figure 1, and the derived Arrhenius parameters are presented in Table 2. Five other studies were performed at room temperature only.<sup>12–16</sup> All results obtained at room temperature are shown in the small inset in Figure 1 and exhibit substantial scattering. Note that the data obtained over wider temperature ranges by Jeong and Kaufman<sup>8</sup> (247–483 K), Taylor et al.<sup>9</sup> (295–800 K), and Herndon et al.<sup>11</sup> (224–378 K) appear to exhibit curvature of the Arrhenius plot. Therefore, we

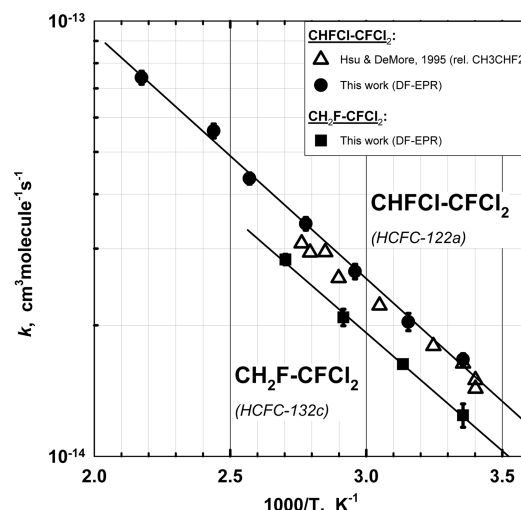


**Figure 2.** Results of rate constant measurements for the reactions of OH with  $\text{CHClCFCl}_2$  (HCFC-122a) and  $\text{CH}_2\text{FCFCl}_2$  (HCFC-132c).  $\text{CHClCFCl}_2$ : (△) Hsu and DeMore,<sup>17</sup> (●) this study.  $\text{CH}_2\text{FCFCl}_2$ : (■) this study. Lines show the results of the least-squares fits to our data.

made three-parameter fits to the entire data sets obtained in these studies and two-parameter fits over restricted temperature intervals for comparison with other available results (see Table 2). The parameters derived from our data are in good agreement with those from Hsu and DeMore<sup>10</sup> (measured between 293 and 358 K) and Herndon et al.<sup>11</sup> (measured between 296 and 398 K). All three of these data sets obtained over similar temperature ranges exhibit very similar temperature dependencies ( $E/R$ ), and the derived  $k_{\text{MC}}(298 \text{ K})$  values span less than 8%. The room-temperature rate constants obtained from all other studies except the very first one<sup>12</sup> exceed the  $k_{\text{MC}}(298 \text{ K})$  obtained in our work and refs 10 and 11 by 20–200%.

**3.1.2.  $\text{CHClCFCl}_2$  (HCFC-122a) and  $\text{CH}_2\text{FCFCl}_2$  (HCFC-132c).** Figure 2 shows the results obtained for both reactions of OH with  $\text{CHClCFCl}_2$  (HCFC-122a) and  $\text{CH}_2\text{FCFCl}_2$  (HCFC-132c). A fit to the data presented in Table 1 for the reaction between OH and  $\text{CHClCFCl}_2$  yields the following Arrhenius expression

$$k_{122a}(298\text{--}460 \text{ K}) = (1.26 \pm 0.24) \times 10^{-12} \exp[-(1298 \pm 66)/T] \text{ cm}^3 \text{ molecule}^{-1} \text{ s}^{-1} \quad (9)$$

The room-temperature rate constant derived from the fit to the entire data set is

$$k_{122a}(298 \text{ K}) = (1.61 \pm 0.07) \times 10^{-14} \text{ cm}^3 \text{ molecule}^{-1} \text{ s}^{-1} \quad (10)$$

The uncertainties in both expressions 9 and 10 are two standard errors from the least-squares fit to the data and do not include the estimated instrumental uncertainty of less than 7%. We found no difference between the results obtained with samples from different makers.

The only other available results for this reaction obtained by Hsu and DeMore<sup>17</sup> are shown in Figure 2 with triangles. There is good agreement between the two data sets. The room-temperature rate constants,  $k_{122a}(298 \text{ K})$ , coincide within statistical uncertainties, and our data exhibit a slightly stronger

**Table 2.** Arrhenius Parameters Derived for OH Reaction Rate Constants Measured in Previous Studies and Those from This Work<sup>a</sup>

$k_i(298\text{ K}) (\times 10^{14} \text{ cm}^3 \text{ molecule}^{-1} \text{ s}^{-1})$	$A (\times 10^{12} \text{ cm}^3 \text{ molecule}^{-1} \text{ s}^{-1})$	$E/R (\text{K})$	temperature range (K)	technique <sup>b</sup>	ref
CH <sub>3</sub> Cl (Methyl Chloride, HCFC-40)					
3.6 ± 0.8			296	DF-LMR	12
8.5			298	CPO	13
4.3 ± 0.36	4.1	1360 ± 130	298–423	FP-RF	6
4.6 ± 0.32	1.75	1085 ± 166	250–350	FP-RF	7
4.1 ± 0.68			297	FP-RA	14
4.25 ± 0.12	$9.25 \times 10^{-14}(T/298)^{3.08}$	$\exp(-232/T)$	247–483	DF-RF	8
4.43 ± 0.20	2.31	1178 ± 78	247–401	DF-RF	8
7.14			300	PR-RA	15
4.16 ± 0.74	$2.48 \times 10^{-13}(T/298)^{2.85}$	$\exp(-285/T)$	295–800	LP-LIF	9
4.99 ± 0.32	1.46	1006 ± 120	295–378	LP-LIF	9
5.3 ± 0.8			298	DF-RF	16
3.37 ± 0.13	4.4	1444 ± 146	293–358	RR, CH <sub>3</sub> CHF <sub>2</sub>	10 <sup>c</sup>
3.63 ± 0.16	$2.08 \times 10^{-13}(T/298)^{2.64}$	$\exp(-520/T)$	224–398	LP-LIF	11
3.63 ± 0.18	4.0	1402 ± 123	298–398	LP-LIF	11
3.59 ± 0.22	2.06	1206 ± 92	224–299	LP-LIF	11
3.43 ± 0.18	3.90 ± 0.94	1411 ± 85	298–460	DF-EPR	this work
CHFCl–CFCl <sub>2</sub> (HCFC-122a)					
1.57 ± 0.05	0.73 ± 0.2	1143 ± 83	294–362	RR, CH <sub>3</sub> CHF <sub>2</sub>	17 <sup>c</sup>
1.61 ± 0.07	1.26 ± 0.2	1298 ± 66	298–460	DF-EPR	this work
CH <sub>2</sub> F–CFCl <sub>2</sub> (HCFC-132c)					
1.23 ± 0.04	0.81 ± 0.2	1247 ± 89	298–370	DF-EPR	this work

<sup>a</sup>Uncertainties are two standard errors from the least-squares fits to the reported data and do not include any systematic uncertainty. <sup>b</sup>Experimental techniques: DF, discharge flow; FP, flash photolysis; LP, laser pulse photolysis; PR, pulse radiolysis; LMR laser magnetic resonance; RF, resonance fluorescence; RA, resonance absorption; LIF, laser-induced fluorescence; EPR, electron paramagnetic resonance spectroscopy; RR, relative rate technique followed by the reference compound; CPO, competitive photo-oxidation. <sup>c</sup>Relative rate results were recalculated using the current recommendations for the rate constants of reference reactions.<sup>2</sup>

temperature dependence. Similar good agreement between results from two groups was previously obtained for the OH reaction with another isomer of this molecule, CHCl<sub>2</sub>CF<sub>2</sub>Cl (HCFC-122).<sup>4,18</sup>

A fit to the data presented in Table 1 for the reaction between OH and CH<sub>2</sub>FCFCl<sub>2</sub> yields the following Arrhenius expression

$$k_{132c}(298\text{--}370\text{ K}) = (8.1 \pm 2.2) \times 10^{-13} \exp[-(1247 \pm 89)/T] \text{ cm}^3 \text{ molecule}^{-1} \text{ s}^{-1} \quad (11)$$

The room-temperature rate constant derived from the fit to the entire data set is

$$k_{132c}(298\text{ K}) = (1.23 \pm 0.04) \times 10^{-14} \text{ cm}^3 \text{ molecule}^{-1} \text{ s}^{-1} \quad (12)$$

The uncertainties in both expressions 11 and 12 are two standard errors from the least-squares fit to the data and do not include the estimated instrumental uncertainty of less than 7%. To the best of our knowledge, no other data on this reaction rate constant are available.

Note that both  $k_{122a}(T)$  and  $k_{132c}(T)$  have very similar values for  $E/R$ , with  $k_{132c}(T)$  being ~33% smaller. We also found that the OH reaction with a CHFCl– reactive group exhibits the same temperature dependence ( $E/R$ ) independent of the nonreactive halogenated tail (–CF<sub>3</sub>, –CF<sub>2</sub>Cl, CFCl<sub>2</sub>, –CF<sub>2</sub>CF<sub>2</sub>Cl).<sup>2</sup> The rate constant decreases slightly with increasing fluorination of the adjacent carbon, whereas the temperature dependence stays unchanged.

### 3.2. UV Absorption Cross Sections of HCFCs.

Absorption cross sections measured for six Cl-containing alkanes are listed in Table 3 with a 2-nm step. Such a presentation is adequate for these smooth spectra; detailed spectra are available upon request. Spectra of four of these compounds (HCFC-122a, HCFC-132c, HCFC-122, and HCFC-123a) were measured for the first time in this work and are shown as solid lines in Figure 3, together with spectra of CHF<sub>2</sub>Cl (HCFC-22), CHFCl–CF<sub>3</sub> (HCFC-124), and CF<sub>2</sub>Cl–CF<sub>2</sub>Cl (CFC-114), which were added for comparison (dashed lines). Figure 4 illustrates the difference between the UV absorption spectrum of CHCl<sub>2</sub>–CF<sub>3</sub> (HCFC-123) obtained in this study and that recommended in JPL Publication 10-6.<sup>2</sup>

**3.2.1. CHFCl–CFCl<sub>2</sub> (HCFC-122a) and CHF<sub>2</sub>–CFCl<sub>2</sub> (HCFC-132c).** No other data on UV absorption of these compounds are available. Their absorption spectra are very similar in both intensity and shape because of the presence of the same CFCl<sub>2</sub> group. The absorption cross sections of CHFCl–CFCl<sub>2</sub> are predictably larger (20–70%) because of additional absorption by the CHFCl group.

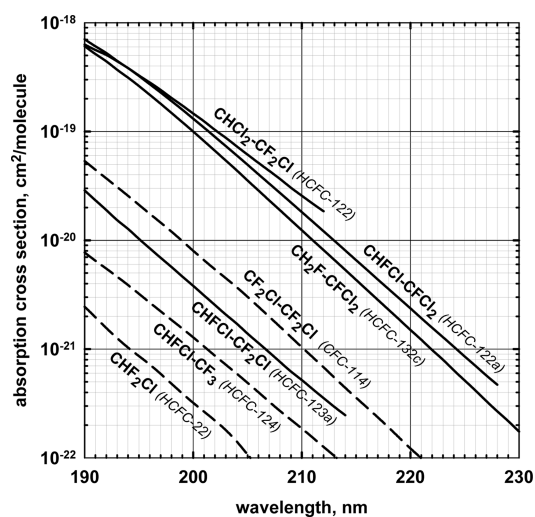
**3.2.2. CHCl<sub>2</sub>–CF<sub>2</sub>Cl (HCFC-122).** No data on the UV absorption of this compound have previously been reported. The intensity of UV absorption of CHCl<sub>2</sub>–CF<sub>2</sub>Cl is consistent with that of molecules containing two Cl atoms at the same methyl group. However, its absorption cross sections do not decrease with increasing wavelength as quickly as those of HCFC-122a and HCFC-132c. Unfortunately, we could not make reliable measurements at longer wavelengths because of the low vapor pressure of the compound.



Table 3. UV Absorption Cross Sections of Cl-Containing Halogenated Alkanes at 295 K<sup>a,b</sup>

wavelength (nm)	CHCl <sub>2</sub> CF <sub>2</sub> Cl (HCFC-122)	CHFClCFCl (HCFC-122a)	CHFClCF <sub>2</sub> Cl (HCFC-123a)	CH <sub>2</sub> FCFCl <sub>2</sub> (HCFC-132c)	CHCl <sub>2</sub> CF <sub>3</sub> (HCFC-123)	CH <sub>3</sub> CFCl <sub>2</sub> (HCFC-141b)
190	63.1	70.5	2.877	60.9	58.8 (−6%) <sup>b</sup>	87.6 (+5%) <sup>b</sup>
192	50.6	52.7	1.896	44.2	43.2	67.4
194	38.3	38.3	1.272	31.3	31.15	49.9
196	28.2	27.2	0.843	21.8	22.06	35.8
198	20.4	19.06	0.569	14.8	15.36	25.1
200	14.6	13.12	0.381	10.0	10.65 (−12%) <sup>b</sup>	17.2 (+4%) <sup>b</sup>
202	10.35	8.93	0.254	6.65	7.29	11.56
204	7.32	6.04	0.172	4.40	5.00	7.68
206	5.16	4.05	0.114	2.87	3.39	5.01
208	3.66	2.72	0.0761	1.89	2.29	3.28
210	2.57	1.82	0.0519	1.238	1.56 (−17%) <sup>b</sup>	2.14 (−1%) <sup>b</sup>
212	1.85	1.21	0.0355	0.814	1.047	1.38
214	1.36	0.806	0.0247	0.535	0.705	0.897
216	1.03	0.536	0.0173	0.350	0.474	0.579
218		0.356	0.0123	0.229	0.317	0.374
220		0.237	0.0088	0.1500	0.213 (−25%) <sup>b</sup>	0.239 (−4%) <sup>b</sup>
222		0.157		0.0980	0.144	0.154
224		0.105		0.0638	0.096	0.0994
226		0.070		0.0415	0.066 (−35%) <sup>b</sup>	0.0636
228		0.047		0.0268	0.045/0.044 <sup>c</sup>	0.0408
230				0.0175	0.031/0.030 <sup>c</sup>	0.0264
232				0.0114	0.022/0.020 <sup>c</sup>	0.0170
234				0.0074	0.016/0.0136 <sup>c</sup>	0.0112
236				0.0046	0.0106/0.0092 <sup>c</sup>	0.0072
238				0.0030	0.0085/0.0062 <sup>c</sup>	0.0046
240				0.0019	0.0064/0.0042 <sup>c</sup>	0.0032 (−4%) <sup>b</sup>

<sup>a</sup>Units are 10<sup>−20</sup> cm<sup>2</sup> molecule<sup>−1</sup>. <sup>b</sup>Differences between the results of present measurements and values recommended in JPL Publication 10-6<sup>2</sup> are listed as percentages in parentheses. The difference was gradually changed between the indicated points. <sup>c</sup>Italicized values are the absorption cross sections of HCFC-123 obtained by extrapolation from the region of the more reliable measurements between 200 and 225 nm.



**Figure 3.** UV absorption cross sections obtained in this study for CHCl<sub>2</sub>CF<sub>2</sub>Cl (HCFC-122), CHFClCFCl<sub>2</sub> (HCFC-122a), CH<sub>2</sub>FCFCl<sub>2</sub> (HCFC-132c), and CHFClCF<sub>2</sub>Cl (HCFC-123a) (solid lines). Evaluated absorption spectra<sup>2</sup> of CHF<sub>2</sub>Cl (HCFC-22), CHFClCF<sub>3</sub> (HCFC-124), and CF<sub>2</sub>ClCF<sub>2</sub>Cl (CFC-114) (dashed lines) for comparison.

**3.2.3. CHFCl–CF<sub>2</sub>Cl (HCFC-123a).** The only reported UV absorption spectrum of this compound<sup>19</sup> is more intense by a factor of 30–50 between 190 and 200 nm. Such disagreement is probably due to experimental problems, which resulted in inconsistent absorption data for other halogenated alkanes as

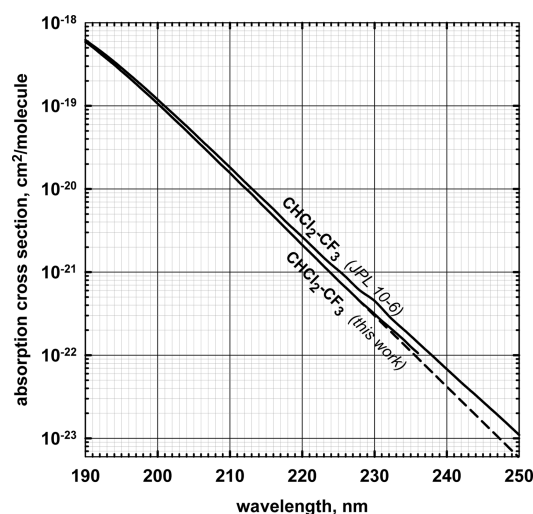


**Figure 4.** UV absorption cross sections of CHCl<sub>2</sub>CF<sub>3</sub> (HCFC-123) obtained in this study and recommended in JPL Publication 10-6.<sup>2</sup> Dashed line is an extrapolation of the fit to the data obtained between 200 and 225 nm (see text).

well. UV absorption by this compound with two adjacent single Cl-containing methyl groups is predictably weaker (more than an order of magnitude) than absorption by CHFCl–CFCl<sub>2</sub> and stronger than absorption by CHFCl–CF<sub>3</sub> (see Figure 3). However, absorption by CHFCl–CF<sub>2</sub>Cl is surprisingly weaker (blue-shifted) than absorption by the more fluorinated CF<sub>2</sub>Cl–CF<sub>2</sub>Cl.

**3.2.4.  $\text{CHCl}_2\text{--CF}_3$  (HCFC-123),  $\text{CH}_3\text{--CFCl}_2$  (HCFC-141b).** These compounds have been intensively studied as CFC substitutes, and their evaluated absorption cross sections were presented in JPL Publication 10-6.<sup>2</sup> Our measurements indicate noticeably lower absorption cross sections for  $\text{CHCl}_2\text{--CF}_3$ , with the difference gradually increasing from ~6% at 190 nm to ~35% at 226 nm and remaining the same at longer wavelengths. However, these longest-wavelength results were obtained only with the highest pressure of the sample, and no test experiment could be performed because of the very low absorption. They seem to be somewhat overestimated at the very long wavelength tail of the spectrum above 230 nm. Therefore, we used a fit to more reliable data measured with larger absorption between 200 and 225 nm,  $\log \sigma(\lambda) = -1.873 - 0.0854\lambda$ , to obtain the extrapolated values at the absorption tail. These extrapolated data are shown with a dashed line in Figure 4 and with italicized text in Table 3. The difference from the JPL Publication 10-6 recommendation becomes as large as 60% at  $\lambda = 240$  nm.

Our results for  $\text{CH}_3\text{--CFCl}_2$  are more consistent with those recommended; the difference gradually changes from +5.5% at 190 nm to -4.5% at 240 nm. Table 3 shows the differences between our results for these compounds and those recommended in JPL Publication 10-6<sup>2</sup> based on previous studies, with percentage values in parentheses.

**3.2.5. IR Absorption Cross Section of HCFCs.** The main IR absorption bands of these six halogenated ethanes were reported in a previous publication.<sup>20</sup> The original IR absorption cross sections (absorption spectra) are available upon request.

## 4. ATMOSPHERIC IMPLICATIONS

**4.1. OH-Driven Tropospheric Lifetime.** The atmospheric lifetimes of halogenated alkanes due to their reactions with tropospheric hydroxyl radicals,  $\tau_i^{\text{OH}}$ , can be estimated by using a simple scaling procedure that is based on the results of field measurements<sup>21</sup> and detailed atmospheric modeling<sup>22</sup>

$$\tau_i^{\text{OH}} = \frac{k_{\text{MCF}}(272 \text{ K})}{k_i(272 \text{ K})} \tau_{\text{MCF}}^{\text{OH}} \quad (13)$$

where  $\tau_i^{\text{OH}}$  and  $\tau_{\text{MCF}}^{\text{OH}}$  are the lifetimes of the compound under study and of methyl chloroform, respectively, due to reactions with hydroxyl radicals in the troposphere only, and  $k_i(272 \text{ K})$  and  $k_{\text{MCF}}(272 \text{ K}) = 6.14 \times 10^{-15} \text{ cm}^3 \text{ molecule}^{-1} \text{ s}^{-1}$  are the rate constants for the reactions of OH with these substances at  $T = 272 \text{ K}$  given by the expressions 7, 9, and 11 and in ref 2, respectively. The value of  $\tau_{\text{MCF}}^{\text{OH}} = 6.1$  years [accepted in the latest World Meteorological Organization (WMO)/United Nations Environment Programme (UNEP) Ozone Assessment<sup>1</sup>] was obtained from the measured lifetime of MCF of 5.0 years after taking into account an ocean loss of 89 years and a stratospheric loss of 39 years. Thus, based on the results of this study and expression 13, the atmospheric lifetime of  $\text{CHFCICFCl}_2$  (HCFC-122a) and  $\text{CH}_2\text{FCFCl}_2$  (HCFC-132c) can be estimated to be 3.51 and 4.52 years, respectively.

The rate constant for the reaction between OH and  $\text{CH}_3\text{Cl}$  below room temperature can be evaluated based on the consistent results from three studies listed in Table 2 (Hsu and DeMore,<sup>10</sup> Herndon et al.,<sup>11</sup> and this study). We calculate an average room-temperature rate constant from these studies of  $k_{\text{MC}}(298 \text{ K}) = 3.47 \times 10^{-14} \text{ cm}^3 \text{ molecule}^{-1} \text{ s}^{-1}$  and derive  $E/R = 1200 \text{ K}$  as a rounded value from a fit to the data reported by Herndon et al.<sup>11</sup> at below room temperatures. Thus, we

recommend the following expression for this reaction rate constant at the temperatures of atmospheric interest

$$k_{\text{MC}}(220\text{--}298 \text{ K}) = 1.95 \times 10^{-12} \exp(-1200/T) \text{ cm}^3 \text{ molecule}^{-1} \text{ s}^{-1} \quad (14)$$

The atmospheric lifetime of methyl chloride can be estimated based on expressions 13 and 14 to be 1.6 years. This value is slightly larger than that recommended in the 2010 WMO/UNEP Ozone Assessment<sup>1</sup> because our recommended  $k_{\text{MC}}(298 \text{ K})$  value slightly differs from that in JPL Publication 10-6.<sup>2</sup>

**4.2. Stratospheric Photolysis Driven Lifetime and Chlorine Loading Potential.** Both the rate constant of the reaction with OH and the UV absorption spectrum are needed to model the potential impact of a compound's release on Earth's atmosphere including the compound's lifetime, ozone depletion potential (ODP), and global warming potential (GWP). Whereas the reaction with OH dictates the atmospheric lifetime of hydrogen-containing compounds, photolysis can play an important role in their destruction in the stratosphere.

Solar UV radiation that can be absorbed by chlorinated alkanes penetrates to the lower stratosphere only within a relatively narrow "stratospheric transparency window" near 200 nm. The intensity of this radiation increases rapidly with altitude,<sup>23</sup> resulting in a very pronounced altitudinal profile of a compound concentration and thus preventing it from penetrating to higher altitudes<sup>24</sup> and dictating a compound's lifetime in the absence of other atmospheric removal processes. Photolysis in the stratosphere is the major removal process for relatively strong UV-absorbing substances, such as  $\text{CFCl}_3$  (CFC-11),  $\text{CF}_2\text{Cl}_2$  (CFC-12),  $\text{CFCl}_2\text{CF}_2\text{Cl}$  (CFC-113), and  $\text{CF}_3\text{Br}$  (Halon-1301). Photolysis still removes ~80% of weaker-absorbing  $\text{CF}_2\text{ClCF}_2\text{Cl}$  (CFC-114), whereas the reaction with  $\text{O}(^1\text{D})$  also becomes an important stratospheric sink.<sup>25</sup> Therefore, the atmospheric lifetimes of these compounds should correlate with their UV absorption characteristics in the stratosphere. Figure 5 shows the currently accepted atmos-

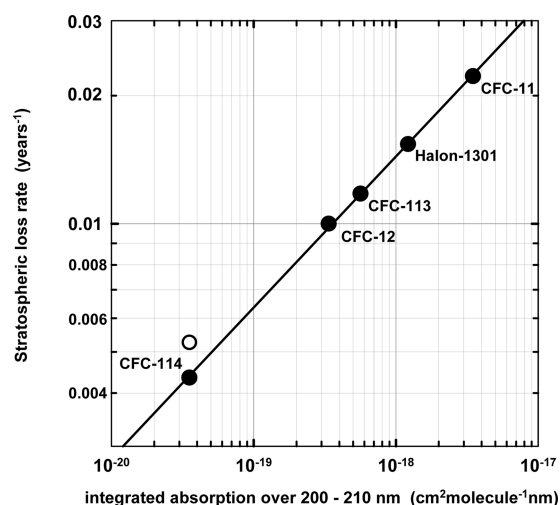


**Figure 5.** Lifetimes of fully halogenated alkanes<sup>1</sup> versus their UV absorption cross sections integrated over 200–210 nm.<sup>2</sup> The line given by eq 15 is the fit to solid circles. The open circle shows the total loss rate of CFC-114, which includes a ~20% contribution from its reaction with  $\text{O}(^1\text{D})$ .

pheric lifetimes<sup>1</sup> of four fully halogenated hydrocarbons (CFC-11, CFC-12, CFC-113, and CFC-114) and Halon-1301 plotted against their UV absorption cross sections integrated over the spectral range between 200 and 210 nm,  $\sigma_{200-210\text{ nm}}$ . This 10-nm-wide wavelength interval was originally chosen to represent the stratospheric transparency window near 200 nm where solar UV radiation penetrates to the lower stratosphere.<sup>23</sup> The solid line is a fit to the data for all five mentioned halocarbons (solid circles) being removed from the atmosphere by stratospheric photolysis. (The open circle shows the total removal rate of CFC-114, whereas its calculated photolysis removal rate<sup>25</sup> is shown with a solid circle.) This dependence can be represented with the expression

$$\log(\tau_{\text{str}}^{\text{ph}}) = -4.55 - 0.355 \log(\sigma_{200-210\text{ nm}}) \quad (15)$$

Note that a Br-containing compound ( $\text{CF}_3\text{Br}$ , Halon-1301) with a very differently shaped UV absorption band, also lies on this line. This good linear correlation reflects the expected variation of the halocarbon lifetime with its UV absorption intensity near 200 nm.

Using expression 15, one can estimate the removal rate due to stratospheric photolysis (stratospheric photolysis lifetime) for partially halogenated alkanes. Column 3 of Table 4 lists the

**Table 4. Stratospheric Photolysis Lifetime ( $\tau_{\text{str}}^{\text{ph}}$ ) and Stratospheric Photolysis Chlorine Loading Potential (SPCLP) of Cl-Containing Alkanes**

molecule (compound)	$\tau^{\text{OH}}$ (years)	$\tau_{\text{str}}^{\text{ph}}$ (years)	SPCLP <sup>a</sup>	ODP <sup>26</sup>	ODP/ SPCLP
$\text{CHCl}_2\text{CF}_2\text{Cl}$ (HCFC-122)	0.96 <sup>c</sup>	79 <sup>d</sup>	0.0099		
$\text{CHFClCFCl}_2$ (HCFC-122a)	3.53 <sup>b</sup>	84 <sup>d</sup>	0.034		
$\text{CHFClCF}_2\text{Cl}$ (HCFC-123a)	4.33 <sup>c</sup>	297 <sup>d</sup>	0.0087		
$\text{CH}_2\text{FCFCl}_2$ (HCFC-132c)	4.55 <sup>b</sup>	94 <sup>d</sup>	0.033		
$\text{CHF}_2\text{Cl}$ (HCFC-22)	11.8 <sup>f</sup>	716 <sup>e</sup>	0.0087	0.034 <sup>f</sup>	3.9
$\text{CHCl}_2\text{CF}_3$ (HCFC-123)	1.4 <sup>f</sup>	86 <sup>e</sup>	0.0098	0.012 <sup>f</sup>	1.2
$\text{CHFClCF}_3$ (HCFC-124)	6.1 <sup>f</sup>	432 <sup>e</sup>	0.0047	0.026 <sup>f</sup>	5.5
$\text{CH}_3\text{CFCl}_2$ (HCFC-141b)	9.2 <sup>f</sup>	77 <sup>e</sup>	0.093	0.086 <sup>f</sup>	0.92
$\text{CH}_3\text{CF}_2\text{Cl}$ (HCFC-142b)	18.5 <sup>f</sup>	424 <sup>e</sup>	0.020	0.043 <sup>f</sup>	2.2
$\text{CHCl}_2\text{CF}_2\text{CF}_3$ (HCFC-225ca)	2.1 <sup>f</sup>	75 <sup>e</sup>	0.0126	0.017 <sup>f</sup>	1.4
$\text{CHFClCF}_2\text{CF}_2\text{Cl}$ (HCFC-225cb)	6.2 <sup>f</sup>	224 <sup>e</sup>	0.0125	0.017 <sup>f</sup>	1.4

<sup>a</sup>From eq 16. <sup>b</sup>From eq 13 using data from this study. <sup>c</sup>From eq 13 using data from JPL Publication 10-6.<sup>2</sup> <sup>d</sup>From eq 15 using data from this study. <sup>e</sup>From eq 15 using data from JPL Publication 10-6.<sup>2</sup> <sup>f</sup>Both atmospheric lifetime and model-calculated ODP are from the same 1998 WMO/UNEP Ozone Assessment 1998<sup>26</sup> for consistency.

$\tau_{\text{str}}^{\text{ph}}$  values of Cl-containing alkanes calculated with expression 15. These photolysis lifetimes are substantially longer than the lifetimes due to reactions with OH in the troposphere (listed in column 2 of Table 4), which thus dictate the total atmospheric lifetimes of these compounds.

Although stratospheric photolysis makes a very minor contribution to the removal of the compound in the

atmosphere, it releases Cl atoms in the stratosphere, thus initiating the chain reaction of ozone depletion. The larger the relative rate of stratospheric photodissociation, the larger the stratospheric chlorine loading and the greater the expected ozone depletion due to the release of the compound. We introduce the stratospheric photolysis chlorine loading potential (SPCLP) as a measure of the chlorine loading to the stratosphere by photolysis of a compound

$$\text{SPCLP} = \frac{(\tau_{\text{str}}^{\text{ph}})^{-1}}{(\tau^{\text{OH}})^{-1} + (\tau_{\text{str}}^{\text{ph}})^{-1}} \frac{M_{\text{CFC-11}}}{M} \frac{n}{3} \quad (16)$$

where  $\tau^{\text{OH}}$  and  $\tau_{\text{str}}^{\text{ph}}$  are the lifetimes of the compound under study due to its reaction with tropospheric OH and due to stratospheric photolysis, respectively;  $n$  is the number of Cl atoms in the molecule; and  $M$  and  $M_{\text{CFC-11}} = 137.5$  are molecular masses of the compound and CFC-11, respectively. We normalized this parameter by the number of Cl atoms and molecular weight of CFC-11 to make it consistent with the ODP formalism.  $\text{SPCLP}_{\text{CFC-11}} = 1$  simply because  $(\tau_{\text{CFC-11}}^{\text{OH}})^{-1} = 0$  and the entire amount of ground-emitted CFC-11 will penetrate the stratosphere to be photolyzed and release Cl atoms. Thus defined, SPCLP should provide a lower-limit estimation of ODP for a compound that is well mixed in the troposphere because  $\tau_{\text{str}}^{\text{ph}}$  characterizes only stratospheric photolysis whereas other processes resulting in stratospheric release of Cl are neglected.

Although partially halogenated compounds react with OH, this removal process is much slower in the stratosphere than in the troposphere because of smaller compound concentrations (due to barometric distribution at least) and smaller reaction rate constants at low stratospheric temperatures. Nevertheless, the reaction with OH in the stratosphere can substantially contribute to stratospheric Cl release and, therefore, to a compound's ODP. Rigorous atmospheric modeling is required to account for all of these processes and calculate ODPs. However, one can compare the available results of atmospheric modeling (ODP values) with the SPCLP values calculated using expression 16. The available model-calculated ODPs of seven HCFCs are presented in the lower part of Table 4. Both the model-calculated ODPs and the total atmospheric lifetimes used in these calculations were taken from the same 1998 WMO/UNEP Ozone Assessment<sup>26</sup> for consistency. The last column of Table 4 shows that the ODPs exceed our SPCLPs calculated with the same input data. Nevertheless, the difference is not very large for compounds with shorter stratospheric photolysis times (i.e., stronger photolysis removal). This difference is substantially larger for compounds with weak UV absorption (containing a single Cl atom), as expected, because of the larger role of other stratospheric processes. It should be noted, that even for stronger UV-absorbing compounds, the reasonable agreement between the ODP and SPCLP values does not mean that photolysis is the major removal process in the stratosphere. Stratospheric reactions and photolysis both change a compound's vertical distribution in the stratosphere, and thus, they affect each other. However, one can conclude that that in case of relatively long-lived compounds (i) SPCLP still can be considered as a lower-limit estimate for ODP and (ii) SPCLP can provide a reasonably good estimate of ODP in some cases of compounds with strong UV absorption and relatively low reactivity toward OH.



## ■ AUTHOR INFORMATION

## Corresponding Author

\*E-mail: vladimir.orkin@nist.gov.

## Present Addresses

<sup>§</sup>Department of Chemistry, University of Leuven, Celestijnenlaan 200 F, 3001 Leuven, Belgium.

<sup>||</sup>American University of Armenia, 40 Marshal Baghramian Ave., Yerevan 0019, Armenia.

## Notes

The authors declare no competing financial interest.

<sup>&</sup>Deceased.

## ■ ACKNOWLEDGMENTS

This work was supported by the Russian Basic Research Foundation, Grant 93-03-112358, and the Upper Atmosphere Research Program of the National Aeronautics and Space Administration. V.G.H. acknowledges the support of Special Foundation of Russian Academy of Sciences, Research Grant, 1993 A3.03. V.L.O. acknowledges the support of NATO CLG Program, Grants ESP.EAP.CLG.983035 and EST.CLG979421.

## ■ REFERENCES

- (1) *Scientific Assessment of Ozone Depletion: 2010*; Global Ozone Research and Monitoring Project—Report No. 52; World Meteorological Organization (WMO): Geneva, Switzerland, 2011.
- (2) Sander, S. P.; Friedl, R. R.; Abbatt, J. P. D.; Barker, J. R.; Burkholder, J. B.; Golden, D. M.; Kolb, C. E.; Kurylo, M. J.; Moortgat, G. K.; Wine, P. H.; Huie, R. E.; Orkin, V. L. *Chemical Kinetics and Photochemical Data for Use in Atmospheric Studies, Evaluation No. 17*; JPL Publication 10-6; Jet Propulsion Laboratory: Pasadena, CA, 2011; available at <http://jpldataeval.jpl.nasa.gov>.
- (3) Certain commercial equipment, instruments, or materials are identified in this article in order to adequately specify the experimental procedure. Such identification does not imply recognition or endorsement by the National Institute of Standards and Technology, nor does it imply that the material or equipment identified are necessarily the best available for the purpose.
- (4) Orkin, V. L.; Khamaganov, V. G. Determination of Rate Constants for Reactions of Some Hydrohaloalkanes with OH Radicals and Their Atmospheric Lifetimes. *J. Atmos. Chem.* **1993**, *16*, 157–167.
- (5) Orkin, V. L.; Kasimovskaya, E. E. Ultraviolet Absorption Spectra of Some Br-Containing Haloalkanes. *J. Atmos. Chem.* **1995**, *21*, 1–11.
- (6) Perry, R. A.; Atkinson, R.; Pitts, J. N., Jr. Rate Constants for the Reaction of OH Radicals with  $\text{CHFCl}_2$  and  $\text{CH}_3\text{Cl}$  Over the Temperature Range 298–423 K, and with  $\text{CH}_2\text{Cl}_2$  at 298 K. *J. Chem. Phys.* **1976**, *64*, 1618–1620.
- (7) Davis, D. D.; Machado, G.; Conaway, B.; Oh, Y.; Watson, R. A. Temperature Dependent Kinetics Study of the Reaction of OH with  $\text{CH}_3\text{Cl}$ ,  $\text{CH}_2\text{Cl}_2$ ,  $\text{CHCl}_3$ , and  $\text{CH}_3\text{Br}$ . *J. Chem. Phys.* **1976**, *65*, 1268–1274.
- (8) Jeong, K.-M.; Kaufman, F. Kinetics of the Reaction of Hydroxyl Radical with Methane and with Nine Cl- and F-Substituted Methanes. I. Experimental Results, Comparisons, and Applications. *J. Phys. Chem.* **1982**, *86*, 1808–1814.
- (9) Taylor, P. H.; D'Angelo, J. A.; Martin, M. C.; Kasner, J. H.; Dellinger, B. Laser Photolysis/Laser-Induced Fluorescence Studies of Reaction Rates of OH with  $\text{CH}_3\text{Cl}$ ,  $\text{CH}_2\text{Cl}_2$ , and  $\text{CHCl}_3$  Over an Extended Temperature Range. *Int. J. Chem. Kinet.* **1989**, *21*, 829–846.
- (10) Hsu, K.-J.; DeMore, W. B. Rate Constants for the Reactions of OH with  $\text{CH}_3\text{Cl}$ ,  $\text{CH}_2\text{Cl}_2$ ,  $\text{CHCl}_3$ , and  $\text{CH}_3\text{Br}$ . *Geophys. Res. Lett.* **1994**, *21*, 805–808.
- (11) Herndon, S. C.; Gierczak, T.; Talukdar, R. K.; Ravishankara, A. R. Kinetics of the Reactions of OH with Several Alkyl Halides. *Phys. Chem. Chem. Phys.* **2001**, *3*, 4529–4535.
- (12) Howard, C. J.; Evenson, K. M. Rate Constants for the Reactions of OH with  $\text{CH}_4$  and Fluorine, Chlorine, and Bromine Substituted Methanes at 296 K. *J. Chem. Phys.* **1976**, *64*, 197–202.
- (13) Cox, R. A.; Derwent, A. E. J.; Eggleton, E. J.; Lovelock, J. A. Photochemical Oxidation of Halocarbons in the Troposphere. *Atmos. Environ.* **1976**, *10*, 305–308.
- (14) Paraskevopoulos, G.; Singleton, D. L.; Irwin, R. S. Rates of Hydroxyl Radical Reactions. 8. Reactions with Chlorofluoromethane, Chlorodifluoromethane, Dichlorofluoromethane, 1,1,1-Chlorodifluoroethane, Chloromethane, and Chloroethane at 297 K. *J. Phys. Chem.* **1981**, *85*, 561–564.
- (15) Nielsen, O. J.; Pagsberg, P.; Sillesen, A. Kinetics of the Reaction of OH with Ethane and a Series of Cl- and F-Substituted Methanes at 300–400 K, Studied by Pulse Radiolysis Combined with Kinetic Spectroscopy. In *Proceedings of the Third European Symposium on the Physico-Chemical Behavior of Atmospheric Pollutants*; Riedel Publishing Co.: Dordrecht, The Netherlands, 1984; p 283.
- (16) Brown, A. C.; Canosa-Mas, C. E.; Wayne, R. P. A Kinetic Study of the Reactions of OH with  $\text{CH}_3\text{I}$  and  $\text{CF}_3\text{I}$ . *Atmos. Environ.* **1990**, *24A*, 361–367.
- (17) Hsu, K.-J.; DeMore, W. B. Rate Constants and Temperature Dependences for the Reactions of Hydroxyl Radical with Several Halogenated Methanes, Ethanes, and Propanes by Relative Rate Measurements. *J. Phys. Chem.* **1995**, *99*, 1235–1244.
- (18) DeMore, W. B. Experimental and Estimated Rate Constants for the Reactions of Hydroxyl Radicals with Several Halocarbons. *J. Phys. Chem.* **1996**, *100*, 5813–5820.
- (19) Doucet, J.; Sauvageau, P.; Sandorfy, C. Photoelectron and Far-Ultraviolet Absorption Spectra of Chlorofluoro Derivatives of Ethane. *J. Chem. Phys.* **1975**, *62*, 355–359.
- (20) Orkin, V. L.; Guschin, A. G.; Larin, I. K.; Huie, R. E.; Kurylo, M. J. Measurements of the Infrared Absorption Cross-Sections of Haloalkanes and Their Use in a Simplified Computational Approach for Estimating Direct Global Warming Potentials. *J. Photochem. Photobiol. A: Chem.* **2003**, *157*, 211–222.
- (21) Prinn, R. G.; Huang, J.; Weiss, R. F.; Cunnold, D. M.; Fraser, P. J.; Simmonds, P. G.; McCulloch, A.; Harth, C.; Salameh, P.; O'Doherty, S.; Wang, R. H. J.; Porter, L.; Miller, B. R. Evidence for Substantial Variations of Atmospheric Hydroxyl Radicals in the Past Two Decades. *Science* **2001**, *292*, 1882–1888.
- (22) Spivakovskiy, C. M.; Logan, J. A.; Montzka, S. A.; Balkanski, Y. J.; Foreman-Fowler, M.; Jones, D. B. A.; Horowitz, L. W.; Fusco, A. C.; Brenninkmeijer, C. A. M.; Prather, M. J. Three-Dimensional Climatological Distribution of Tropospheric OH: Update and Evaluation. *J. Geophys. Res.* **2000**, *105*, 8931–8980 and references therein.
- (23) DeMore, W. B.; Golden, D. M.; Hampson, R. F.; Howard, C. J.; Kolb, C. E.; Kurylo, M. J.; Molina, M. J.; Ravishankara, A. R.; Sander, S. P. *Chemical Kinetics and Photochemical Data for Use in Stratospheric Modeling, Evaluation No. 12*; JPL Publication 97-4; Jet Propulsion Laboratory: Pasadena, CA, 1997; p 257; available at [http://jpldataeval.jpl.nasa.gov/pdf/Atmos97\\_Anotated.pdf](http://jpldataeval.jpl.nasa.gov/pdf/Atmos97_Anotated.pdf).
- (24) *Atmospheric Ozone 1985. Assessment of Our Understanding of the Processes Controlling its Present Distribution and Change*; Global Ozone Research and Monitoring Project—Report No. 16; World Meteorological Organization (WMO): Geneva, Switzerland, 1985; Vol. 2.
- (25) Prather, M. J.; Hsu, J.  $\text{NF}_3$ , the Greenhouse Gas Missing from Kyoto. *Geophys. Res. Lett.* **2008**, *35*, L12810. Prather, M. J.; Hsu, J.  $\text{NF}_3$ , the Greenhouse Gas Missing from Kyoto. *Geophys. Res. Lett.* **2010**, *37*, L11807.
- (26) *Scientific Assessment of Ozone Depletion: 1998*; Global Ozone Research and Monitoring Project—Report No. 44; World Meteorological Organization (WMO): Geneva, Switzerland, 1999.